JOURNAL OF MATERIALS SCIENCE 26 (1991) 2026–2030

Stability of zirconia–ceria–yttria ceramics in hostile environments

C. LEACH, N. KHAN
Department of Materials, Imperial College of Science, Technology and Medicine, Prince Consort Road, London SW7 2BP, UK

The phase chemistry, conductivity in air and forming gas, and stability in warm humid environments of zirconia–ceria–yttria ceramics are described. The compositions studied lie between 12 mol% ceria/88 mol% zirconia and 3 mol% yttria/97 mol% zirconia and fall within the tetragonal phase field of this ternary system. At temperatures below 700 °C, reducing atmospheres were found to affect only the conductivity of the end-member ceria–zirconia ceramic, having no effect on the ternary compositions investigated. Compositions containing more than 10 mol% ceria were found to be more stable to stabilizer loss in water vapour at 132 °C than those containing less than 10 mol% ceria.

1. Introduction

Submicrometre grain size, tetragonal-phase yttria–zirconia ceramics (Y–TZP) are well known for their high modulus of rupture and fracture toughness [1], as well as their good anionic transport properties at moderate temperature [2, 3]. Their properties are exploited in areas as diverse as wear components and solid electrolytes [4, 5]. However, the application of these ceramics is not without problems: destabilization by yttria leaching is rapid in humid environments above room temperature [6, 7], the fine grain size can lead to creep problems at high temperature [8], and chemical unmixing to yield the cubic and monoclinic phases occurs during long anneals at high temperature [9]. Further, the fracture behaviour of Y–TZP shows a less pronounced *R*-curve than ceramics in other stabilized zirconia systems, notably $MgO–ZrO_2$ or $CeO_2–ZrO_2$, and so is likely to have poorer fatigue resistance in situations where the ceramic is subcritically loaded [10].

The microstructure of tetragonal $CeO_2–ZrO_2$ ceramics (Ce–TZP) is, in many respects, similar to that of Y–TZP, but with a larger critical grain size, requiring more grain growth before optimum toughness is achieved [11]. The larger grain size also leads to a reduction in the specific grain-boundary area of the ceramic which is desirable in electrolyte applications where a high resistivity, low ionic mobility, glassy grain-boundary phase is generally present [12]. Ce–TZP shows strong *R*-curve behaviour and is relatively stable in humid environments [13]. However, it suffers from poor ionic conductivity because the substitution of zirconium by tetravalent cerium does not result in the generation of oxygen site vacancies within the fluorite-type lattice; a feature which is essential for enhanced oxygen ion conductivity. As a consequence, the ionic conductivity of Ce–TZP containing 12 mol% ceria (12Ce–TZP) at 700 °C is two orders of magnitude poorer than 3Y–TZP. Further, cerium shows variable valency under certain conditions, changing readily from the fully oxidized tetravalent state to trivalency or divalency by an electron hopping mechanism [14]. The consequences of this reduction potentially lead to mechanical and electrical stability problems in a reducing environment at elevated temperature. In particular there can be an increase in electronic conductivity associated with the variations in valency, a phenomenon which would be undesirable in electrolyte applications where the maximization of oxygen migration rates is critical.

Thus both Y–TZP and Ce–TZP are seen to have specific advantages and disadvantages when considered for use in hostile environments or electrolyte applications. The purpose of this work is to attempt to identify ternary Y–Ce–TZP compositions which retain the better aspects of the binary TZPs specific to certain applications. To this end, the properties of end member and intermediate compositions along the tie-line joining 3Y–TZP to 12Ce–TZP have been investigated, with particular reference to ionic transport properties and chemical stability. The majority of these compositions fall within the predominantly single-phase tetragonal phase field at typical sintering temperatures, say 1500 °C, but those at the yttrium-rich end of the tie line may lie within the two-phase tetragonal plus cubic field, and hence develop a microstructure where a secondary cubic or t′ phase is present in an amount dependent on the precise sintering conditions [15].

2. Experimental procedure

Ternary Y–Ce–TZP ceramic powders were prepared by mechanically mixing commercially available 3Y–TZP and 12Ce–TZP powders (Tosoh Inc., Japan) in such proportions as to yield compositions along the tie-line corresponding to 2, 4 and 8 mol% CeO_2 (see Fig. 1). The powders were milled in methanol for 24 h

0022–2461/91 $03.00 + .12

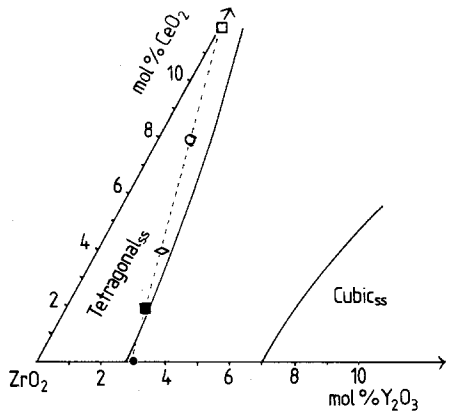

Figure 1 Ternary section through the proposed ZrO_2–CeO_2–Y_2O_3 phase diagram showing the sample compositions selected for this study. (See also [19].) (□) A, (○) B, (◇) C, (■) D, (●) E.

and evaporated to dryness, then seived through a 38 μm seive to break up large agglomerates. Compacts of these and the end-member compositions were pressed and isopressed at 200 MPa and sintered in air at 1550 °C for 5 h. X-ray analysis of the sintered ceramics showed them to comprise predominantly tetragonal zirconia with steadily increasing lattice parameters as the ceria content was increased.

In order to establish the stability of these compositions to prolonged exposure to a reducing atmosphere at elevated temperature, samples of each composition measuring 6 mm × 6 mm × 20 mm were aged for 500 h at 1000 °C in an atmosphere furnace containing a 10% H_2/N_2 mixture. The bars were then sectioned and the centres examined in the scanning electron microscope (SEM).

X-ray phase determination was carried out on a Phillips diffractometer and processed using an in-house peak stripping and smoothing program. Quantification of the phases present was by peak-area measurement using the calibration of Toraya *et al.* [16, 17] for binary TZPs.

The electrical behaviour of each composition was measured, both in air and a reducing atmosphere (10% H_2/N_2 mixture) at temperatures up to 700 °C, by a.c. impedance spectroscopy using a Hewlett Packard 4192A LF impedance analyser. Samples were allowed to equilibrate with the gas for 1 h prior to measurements being made. This approach was used to look for conductivity variations in samples arising from changes in the enveloping atmosphere. It is believed that this can lead to changes in cerium valency within the lattice which can increase the electronic component of conductivity of the ceramic, reducing the percentage contribution to the total conductivity of the ionic transport processes.

Corresponding values for A and E_A in the Nernst equation

$$\sigma T = A\exp(-E_A/kT)$$

were calculated.

Finally, the stability of the ceramics in humid environments was determined. The test pieces were maintained in an autoclave at 132 °C in saturated water vapour at 1.6 bar for periods up to 12 h and the development of monoclinic phase on the surface quantified by X-ray diffraction.

3. Results

3.1. Scanning electron microscopy

Table I lists the measured grain sizes of the ternary samples and Fig. 2 comprises typical microstructures from polished and thermally etched sections through the sintered bodies. Although the sintering conditions for each sample were identical, the grains are seen to increase in size as the ceria content of the ceramic is increased. The reducing heat treatment had no measurable effect on grain size. All samples were 96% to 98% dense with residual porosity confined to the ceramic grain boundaries for pore diameters greater than 0.5 μm. In the ceria-rich samples many of the grain boundaries were wavy, illustrating disequilibrium and indicating that grain growth was still rapid at the end of the firing cycle.

3.2. X-ray diffraction

The lattice parameters of the ceramics investigated here are listed in Table II. It can be seen that, as the mole fraction of the larger (than Y^{3+}) cerium(IV) ion incorporated in the lattice is increased, both the lattice parameters and the c/a ratio increase in sympathy. Analysis of the diffraction patterns shows that, except in the case of the 3Y–TZP where ~ 5 vol % of a non-transformable secondary tetragonal phase is also present (see [15]), the ceramics contain in excess of 98% of a primary tetragonal phase.

3.3. Electrical properties

Arrhenius plots showing a.c. impedance data from the ceramic pieces tested in air and forming gas are shown in Fig. 3; Table III lists values for the pre-exponential factors, A, and activation energies, E_A, derived from fitting the Nernst equation to the measured bulk conductivities. It can be seen that, for all compositions apart from the 12 mol % ceria–zirconia binary, there is a negligible effect on the samples' conductivities due to the differences in atmosphere surrounding the test pieces, at temperatures below 700 °C. The behaviour of the 12 mol % ceria–zirconia binary in the reducing atmosphere shows a much steeper slope above 350 °C with superior conductivity to the other samples at temperatures over 600 °C. This difference is likely to be due to the incorporation of a component of electronic conductivity arising from the reduction of some

TABLE I Measured grain sizes of the ceramics after sintering (for composition key see Fig. 1)

Composition	Density (g cm^{-3})	Grain size (μm)
A	6.27	8.5
B	6.22	7.2
C	6.09	1.7
D	6.14	–
E	6.10	0.8

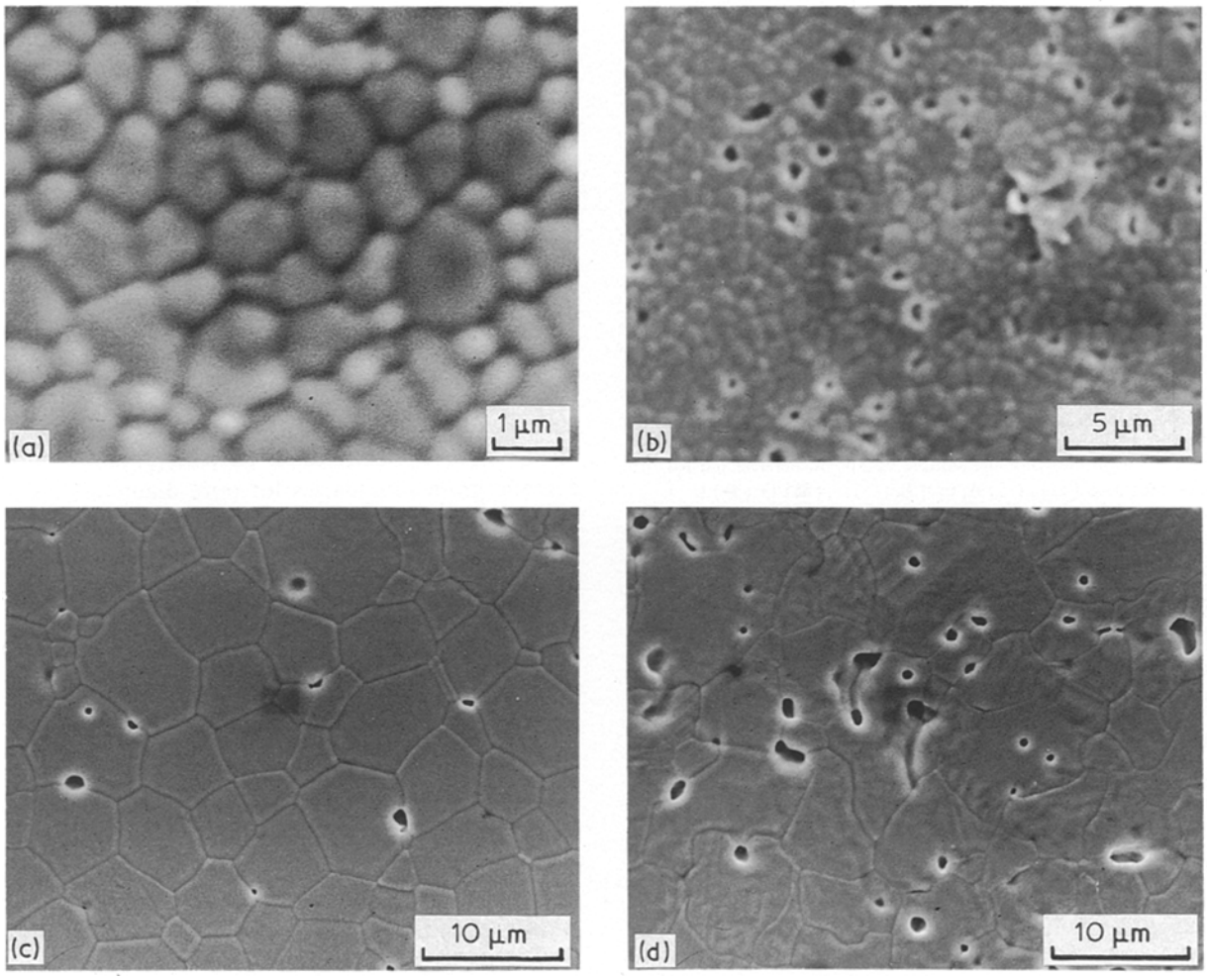

Figure 2 Microstructures of the sintered ceramics. The micrographs correspond to ceramics with ceria contents of (a) 0 mol %, (b) 4 mol %, (c) 8 mol % and (d) 12 mol %, respectively.

TABLE II Measured lattice parameters and c/a ratios of the tetragonal phase after sintering as determined by X-ray diffraction (for composition key see Fig. 1)

Composition	a (nm)	c (nm)	c/a
A	0.513	0.520	1.015
B	0.512	0.517	1.009
C	0.511	0.520	1.019
D	0.510	0.515	1.010
E	0.510	0.514	1.007

TABLE III Pre-exponential (A) and activation energy (E_A) values for bulk conductivity calculated according to the Nernst equation and fitting the data of Fig. 3 (for composition key see Fig. 1)

Composition	Air		Forming gas	
	A (Scm)	E_A (eV)	A (Scm)	E_A (eV)
A	35	1.02	4927	1.16
B	134	0.91	251	0.94
C	244	0.91	244	0.91
D	248	0.90	214	0.88
E	225	0.87	290	0.89

of the cerium from a tetravalent to a trivalent state. We are currently determining the range of conditions under which electronic conductivity is significant in Ce–TZP. No similar behaviour is seen in the ternary compositions at temperatures below 700 °C.

3.4. Stability in humid environments

In all samples, except for those containing 12 mol % ceria, increases in the surface monoclinic content were detected with increasing annealing time. This variation was found to be approximately linear with time (Fig. 4a), with the rate of monoclinic zirconia formation increasing with decreasing ceria content. The increase in monoclinic zirconia after a fixed annealing time was also found to vary approximately linearly with ceria content along this tie-line (Fig. 4b). Extrapolation of the data from Fig. 4b to zero time suggests that the ceramics in this series become insensitive to these conditions of humid environment at a ceria content of $\sim$ 10 mol %.

4. Discussion

The grain-size measurements from ceramic compositions along this tie-line confirm that under identical sintering conditions, grain growth is more pronounced in ceria-rich compositions than yttria-rich. Coupled with the X-ray results, it is inferred that the critical particle size for spontaneous transformation is increased with increasing ceria content. This is in agreement with previous work [11] and results in microstructural variations as a function of composition throughout this series. It is fairly well established that R-curve behaviour is more marked in Ce–TZP

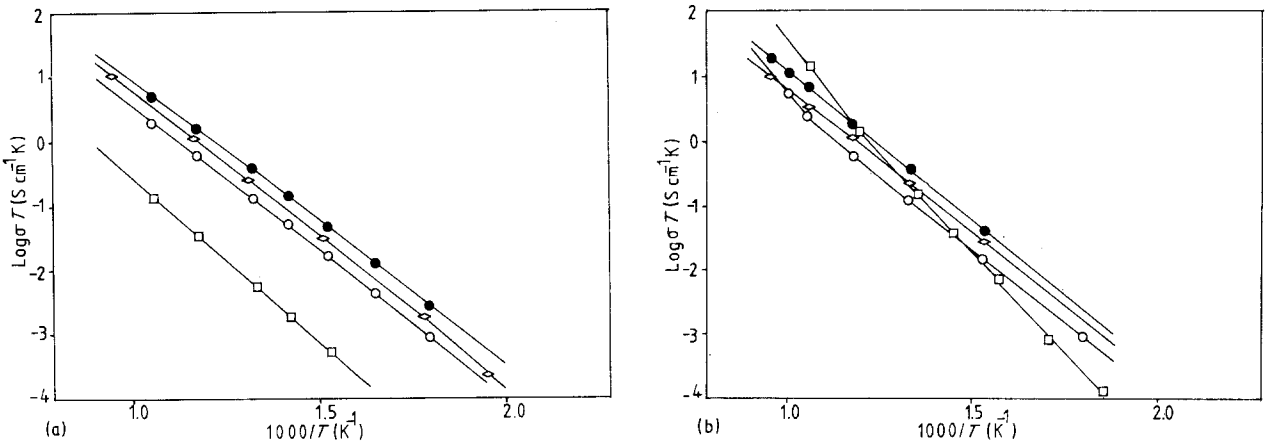

Figure 3 Arrhenius plots showing the variation of bulk ceramic conductivity with temperature for the series as measured in (a) air, and (b) forming gas. For key, see Fig. 1.

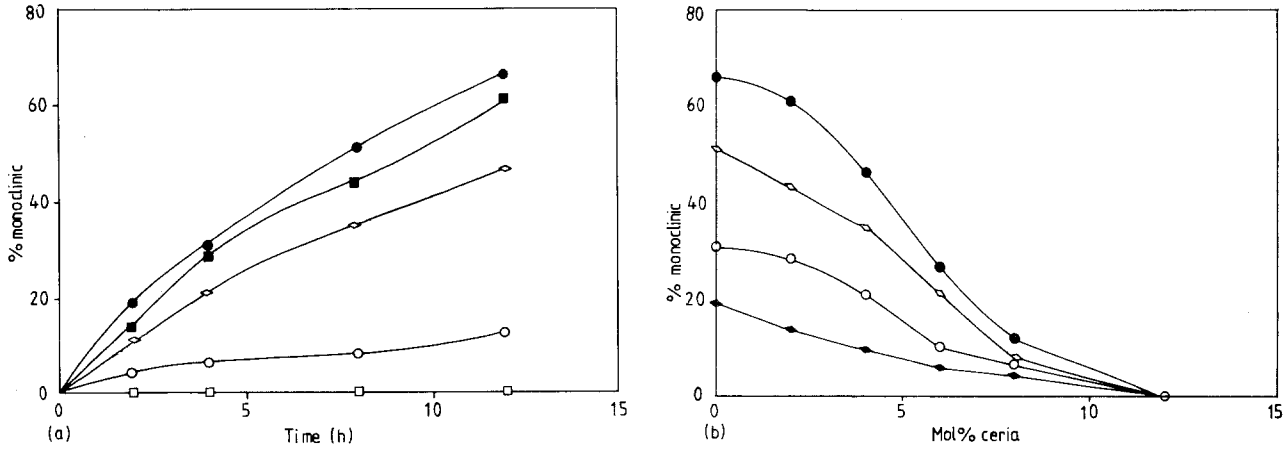

Figure 4 Graphs showing the stability of the series in water vapour at 132 °C. The amount of surface monoclinic zirconia present is plotted (a) as a function of time at constant composition (for key, see Fig. 1) and (b) against ceria content for constant ageing times (●) 12 h, (◇) 8 h, (○) 4 h, (◆) 2 h.

than in Y–TZP and this may lead to differences in subcritical crack growth phenomena. If, under submaximal loading, the rapid growth of small cracks can be discouraged through *R*-curve behaviour, then some tolerance to minor deformations can be introduced into that component without significant risk of structural failure. It may thus be possible to tolerate a certain crack size within a component before other properties are compromised. In contrast, if the ceramic were to be used as a component in a solid state electrochemical reactor, where a typical electrolyte thickness would be of the order of 500 μm, or less, a crack connecting both sides of the electrolyte would seriously affect the efficiency of the electrochemical reactions taking place. Thus an upper limit to microcrack size could be introduced within the ceramic's design criteria, and satisfied by choosing a material with suitable *R*-curve properties. These possibilities are currently being investigated in fatigue experiments designed to nucleate and propagate small cracks under subcritical loads.

Comparison of the electrical impedance data collected in air and forming gas demonstrates that the thermodynamic stability of tetravalent cerium to reduction within the solid solution is improved by the presence of yttrium ions. Patil *et al.* [18] measured ionic transference numbers in 12Ce–3Y-TZP at pressures, $p(O_2)$, down to 10^{-6} atm and temperatures in excess of 1100 K. Their value at 1100 K was 0.9, but this decreased significantly to around 0.6 at higher temperatures. Previous work [19] shows this composition to lie within the two-phase cubic + tetragonal region of the phase diagram. It is thus expected that the conducting species in the ternary compositions are predominantly ionic.

Activation energy values vary from 0.88 to 0.94 eV in the ternary series with higher values being measured in the cerium-rich samples. Theses values are equated with the energy for oxygen vacancy migration and represent the sum of a dissociation and a migration term. The incorporation of ceria into Y–TZP, at levels up to 6 mol %, reduces the bulk conductivity marginally at 800 °C but permits a larger grain size. This has the effect of reducing the component of resistance due to the grain-boundary regions of the ceramic [12]. Thus, in a ternary composition of typical purity, the reduction in bulk conductivity may be compensated for by the increase in grain-boundary conductivity.

The ageing experiments in saturated water vapour at 132 °C demonstrate that at least 10 mol % ceria is required in solid solution in order that the consequent destabilization of the ceramic is effectively halted. At

these ceria levels, it is still possible to incorporate significant amounts of yttria into the solid solution without departing significantly from the tetragonal single-phase field. Thus desirable ionic transport properties in electrolytes in humid environments may be achievable in a TZP ceramic showing pronounced *R*-curve behaviour. Unpublished ESCA analyses [20] of binary and ternary TZP compositions indicates that ceria segregates more strongly to the ceramic grain boundary than yttria in ceria-rich ternary compositions, giving rise to a complete layer of cerium at the ceramic surface. This layer appears to protect the yttrium from reacting with the water vapour to form the hydroxide and remove it from the ceramic.

The above results demonstrate that compositions within the Ce–Y–TZP ternary show combinations of properties which may be considered superior to those of the binary end members. Thus it is important to choose carefully the composition of a TZP ceramic in order that its properties may be optimized for the proposed application.

References

1. R. C. GARVIE, in "Advances in Ceramics", Vol. 12, "Science and Technology of Zirconia II", edited by N. Claussen, M. Ruhle and A. Heuer (The American Ceramic Society, Columbus, Ohio, 1984) pp. 465–79.
2. J. F. BAUMARD and P. ABELARD, *ibid.*, pp. 555–71.
3. C. R. A. CATLOW, in "Non-stoichiometric oxides", edited by O. T. Sorensen (Academic Press, New York, 1981) pp. 61–99.
4. U. DROWAK, H. OLAPINSKI, D. FINGERLE and U. KROHN, in "Advances in Ceramics", Vol. 12, "Science and Technology of Zirconia II", edited by N. Claussen, M. Ruhle and A. Heuer (The American Ceramic Society, 1984) pp. 480–7.
5. B. C. H. STEELE, *Chem. Ind.* (1986) 651.
6. F. F. LANGE, G. L. DUNLOP and B. I. DAVIS, *J. Amer. Ceram. Soc.* **69** (1986) 237.
7. T. SATO and M. SHIMADA, *ibid.* **68** (1985) 356.
8. R. DUCLOS, J. CRAMPON, Y. BIGAY, B. CALES and J. P. TORRE, in "Science of Ceramics", Vol. 14, edited by D. Taylor (Institute of Ceramics, Stoke-on-Trent, England, 1988) pp. 581–6.
9. V. S. STUBICAN and J. R. HELLMANN, in "Advances in Ceramics", Vol. 3, "Science and Technology of Zirconia", edited by L. Hobbs and A. Heuer (The American Ceramic Society, Columbus, Ohio, 1981) pp. 25–36.
10. R. H. DAUSKARDT, W. YU and R. O. RITCHIE, *J. Amer. Ceram. Soc.* **70** (1987) C248.
11. J. G. DUH, H. T. DAI and B. S. CHIOU, *ibid.* **71** (1988) 813.
12. M. T. HERNANDEZ, J. R. JURADO and P. DURAN, *Solid State Ionics*, to be published.
13. T. SATO and M. SHIMADA, *J. Mater. Sci.* **20** (1985) 3988.
14. D. J. M. BEVAN and J. KORDIS, *J. Inorg. Nucl. Chem.* **26** (1964) 1509.
15. C. A. LEACH, *J. Mater. Sci. Lett.* **6** (1987) 303.
16. H. TORAYA, M. YOSHIMURA and S. SOMIYA, *J. Amer. Ceram. Soc.* **67** (1984) C119.
17. *Idem., ibid.* **67** (1984) C183.
18. D. S. PATIL, N. VENKRATAMANI and V. K. ROHATGI, *J. Mater. Sci.* **23** (1988) 3367.
19. N. KHAN, C. LEACH, *Brit. Ceram. Proc.* **42** (1989) 133.
20. C. A. LEACH, unpublished work (1988).

Received 9 June
and accepted 23 October 1989